Plasma Chemistry and Plasma Processing
https://doi.org/10.1007/s11090-019-09984-7

ORIGINAL PAPER

Simultaneous Degradation of Aqueous Trichloroacetic Acid by the Combined Action of Anodic Contact Glow Discharge Electrolysis and Normal Electrolytic Processes at the Cathode

Chen Zhao[1,2] · Haiming Yang[1,2] · Maowei Ju[3] · Xiaotong Zhao[1,2] · Lixiang Li[1,2] · Shaoyan Wang[1] · Baigang An[1,2]

Received: 8 April 2018 / Accepted: 15 March 2019

Abstract
To enhance the removal of trichloroacetic acid (TCA) by anodic contact glow discharge electrolysis (CGDE), the combined degradation of TCA by the action of anodic CGDE, denoted anodic degradation, and normal electrolytic processes at the cathode, denoted cathodic degradation, was investigated. Here, this overall process is termed simultaneous degradation. Compared to anodic degradation, in simultaneous degradation, the reduction rates for TCA and total organic carbon (TOC) increased from 65.32% and 62.03% to 91.82% and 73.03%, respectively. Meanwhile, the dechlorination rate rose from 64.6 to 80.12%. For simultaneous degradation, the disappearance of TCA, the reduction in the TOC, and the dechlorination of TCA, followed first-order kinetics. The reaction intermediates were detected and, based on the intermediates and the observed kinetics, the effects of the simultaneous degradation of TCA, TOC, and dechlorination of TCA are discussed. The cathode materials, length of the anode dipped into the electrolyte, and Pd loading on the Ni cathode all affected the simultaneous degradation of TCA significantly. The effect of the addition of Fe^{2+} was also investigated. The additive and synergistic effects of the combination of anodic and cathodic degradations on simultaneous degradation are discussed. Based on these results, an analysis of the degradation of TCA suggests that ·OH and $\cdot H/e^-_{aq}$ generated by the action of anodic CGDE, as well as the $\cdot H_{ads}$ generated on the Pd-loaded Ni cathode surface, are the key species responsible for the dechlorination of TCA. Furthermore, possible mechanistic routes for the simultaneous degradation of TCA are proposed.

Keywords Simultaneous degradation · Hydroxyl radical · Absorbed hydrogen radical · Anodic CGDE · Trichloroacetic acid · Pd loading

✉ Haiming Yang
yanghaiming80@sina.com

[1] School of Chemical Engineering, University of Science and Technology Liaoning, Anshan 114051, People's Republic of China

[2] Institute of Materials Electrochemistry Research, University of Science and Technology Liaoning, 185 Qianshangzhong Road, Anshan 114051, People's Republic of China

[3] National Marine Environmental Monitoring Center, Dalian 116023, People's Republic of China

Introduction

In the past few decades, the interest in the utilisation of electroprocesses, such as plasma electrolytic oxidation at the anode and electroreduction with a Pd-loaded Ni cathode, for the treatment of wastewater containing persistent organic pollutants (POPs) has increased [1–3]. For example, the exhaustive mineralisation of POPs by plasma electrolytic oxidation and total dehalogenation by electroreduction have been reported [3–5]. Among the plasma electrolytic oxidation processes, anodic contact glow discharge electrolysis (CGDE), which was first named and studied by Hickling [6], is one of the most promising methods. In anodic CGDE, electroplasma is generated close to the anode immersed in an aqueous electrolyte. This electroplasma is the reactive agent for anodic CGDE. Furthermore, anodic CGDE can be observed in normal electrolysis when a voltage higher than 420 V is applied using a thin wire anode immersed in aqueous electrolyte [7]. The cations in the electroplasma are accelerated by the steep potential gradient at the plasma/anolyte solution interface and rush towards the solution, and the energized cations might recombine with other ions and/or electrons resulting the formations of corresponding energetic products. Then, in the liquid-phase anodic reaction zone, which is in the vicinity of the plasma/solution interface, the energetic products break water molecules into ·H and ·OH, as shown in reaction 1 [6–11]. In particular, e^-_{aq} is generated from ·H, as shown in reaction 2 [12]. H_2O_2 is one of the main products of anodic CGDE in solutions of inert electrolytes, and it is formed by the recombination of ·OH, as shown in reaction 3 [13]. Thus, the action of anodic CGDE causes oxidation because of the action of ·OH and reduction via ·H and e^-_{aq} in the liquid-phase anodic reaction zone. The reactions involved in anodic CGDE are denoted anodic degradation here. Because oxidants, mainly ·OH and H_2O_2, are generated in the liquid-phase reaction zone of anodic CGDE, anodic CGDE has been developed as a novel plasma electrolytic oxidation technique [14–28]. During anodic CGDE, although the concentration of H_2O_2 is high, it is still much weaker than that of ·OH. Consequently, based on a series of studies concerning the degradation of POPs, such as aromatic compounds, by anodic CGDE, it has been assumed that ·OH is the key species for the breakdown of benzene moieties [29–32].·H or e^-_{aq} generated in the liquid-phase reaction zone of anodic CGDE have also been investigated to reduce Cr(VI), TCA, and carbon dioxide (CO_2) concentrations [33–35]. To enhance the efficiency of POPs degradation by anodic CGDE, Fe^{2+} and Fe^{3+} have also been added as a Fenton catalysts to enable the utilisation of the H_2O_2 formed in the anodic zone of anodic CGDE, thus converting two H_2O_2 molecules into one ·OH radical [36]. Furthermore, the use of several anodes to increase the yield of ·OH [15] has also been reported. However, unlike the action of anodic CGDE, at the cathode, there is a normal electroreduction process (i.e., a normal electrolytic process). In addition, $\cdot H_{ads}$ is generated by normal electrolytic processes on the surface of Pd-loaded Ni cathode (as shown in reaction 4) [36]. The reductive $\cdot H_{ads}$ species produced by the normal electrolytic process at the cathode has not be employed to degrade POPs, and this process is denoted cathodic degradation here.

$$H_2O \overset{\text{CGDE}}{\rightarrow} \cdot H + \cdot OH \tag{1}$$

$$\cdot H \overset{yH_2O}{\rightarrow} H^+ + e^-_{aq} \quad pK_a = 9.6 \tag{2}$$

$$\cdot OH + \cdot OH \rightarrow H_2O_2 \tag{3}$$

$$e^{-} \underset{\text{Cathode}}{\overset{H^{+}}{\rightarrow}} \cdot H_{ads} \quad (4)$$

TCA, a typical POP, is found in drinking water because of the use of chlorine to treat water (drinking water chlorination). TCA is harmful and carcinogenic [37, 38]. Many treatment technologies, such as biotechnology [39], photocatalysis [40], electroreduction [41], sonolysis [42], radiation [43], and gas discharge [44], as well as combinations of these technologies, has been investigated for the degradation of TCA [45, 46]. However, there are some disadvantages for these technologies. For example, bio-technological techniques can degrade TCA, but, in most cases, the efficiency is low because of the severe toxicity of TCA. Electroreduction can degrade TCA with low power consumption, but the TCA cannot be completely mineralised, resulting in the formation of dichloroacetic acid (DCA), monochloroacetic acid (MCA), and acetic acid (AA) as intermediates. The use of radiation is an efficient way to decompose TCA, but the process is complex and the consumed materials are expensive. The successful dechlorination and decomposition of TCA by the action of anodic CGDE was first reported by Wang [34]. However, reduction induced by the normal electrolytic process at the cathode has not been considered and utilised to degrade TCA.

To enhance the efficiency of anodic CGDE in the treatment of TCA, as well as the treatment of other chlorinated organic compounds, we investigated the simultaneous degradation of TCA by combining the action of the anodic CGDE and that of the normal electrolytic process occurring at the cathode in a process that we call 'simultaneous degradation'. The additive and synergistic effects of the combination of the anodic and cathodic degradation processes on the simultaneous degradation of TCA and TOC, as well as the dechlorination of TCA, are discussed and possible mechanistic routes for the simultaneous degradation of TCA are proposed.

Experimental

Materials

Cu and Ni plates were purchased from Baojishi Pengshengxin No Ferrous Metal Co., Ltd. The cation exchange membrane used in this study was Nafion 117 (N117, Techno-Sigma Co., Okayama, Japan). The above materials were all used as received. $PdCl_2$ (99.5%) was obtained from Sinopharm Chemical Reagent Co., Ltd. TCA (99%) was obtained from Shanghai Jingchun Scientific Co., Ltd.

Apparatus and Procedures

Figure 1i shows the reaction apparatus and assembly for the anodic degradation of TCA by the action of anodic CGDE. A cylindrical glass cell (48 mm in inner diameter) was employed. The anode from which the discharge was emitted was a pointed platinum wire (0.6 mm in diameter) that was placed into the cell. The capacity of the cell was 100 mL, and the volume of the reaction solution in the cell was 70 mL. The cathode was a Pd-loaded Ni plate (working size 20×20×1.5 mm) placed in another glass tube, the lower end of which was plugged with Nafion N117 membrane, thus allowing only the passage of electrons, separating the cathodic and anodic zones, and preventing the transfer of TCA

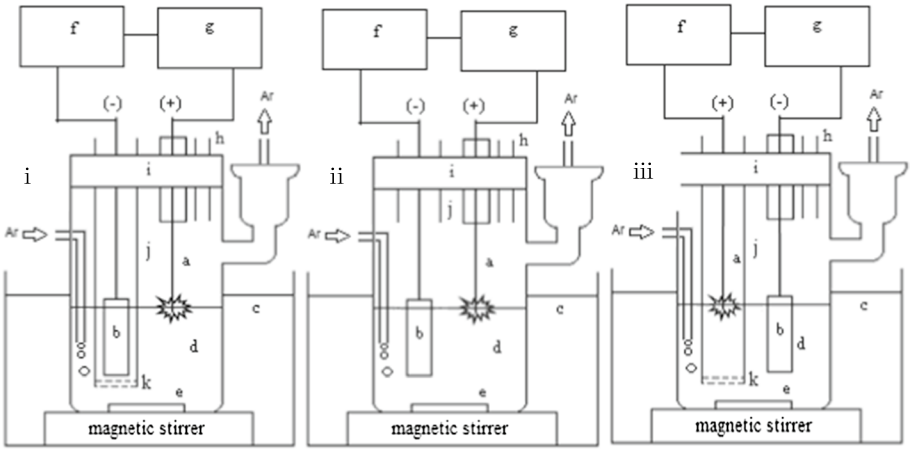

Fig. 1 Left to right: Apparatus for cathodic degradation (**i**), simultaneous degradation (**ii**), and cathodic degradation (**iii**). a: Anode; b: cathode; c: ice–water bath; d: electrolytic solution; e: Teflon-coated magnet bar; f: digital coulometer; g: DC power supplier; h: sampling hole; i: rubber plug; j: glass tube; and k: Nafion N117 membrane

between these zones. The capacity of the glass tube sealed by N117 was 5 mL, and the electrolyte was aqueous 20 mM sodium sulfur (5 mL). The Pd-loaded Ni cathodes were prepared by electroless deposition [47]. Reagent grade TCA was purchased and used as received and dissolved in aqueous 20 mM sodium sulfur. The height of the aqueous solution in the cell was approximately 3.9 mm, corresponding to about 70 mL substrate solution with a pH_0 of 2.8. A voltage of 500 V from a direct current (DC) power supply (ELEPOS PS-1510) was applied between both electrodes to start the run. The depth of the discharge electrode (anode) dipped into solution was adjusted so that the average current was 70 mA, i.e., approximately 2.0 mm. The total amount of electricity passing during electrolysis was monitored using a digital coulometer (Hokuto Denko HF-201). The solution was stirred gently with a magnetic bar covered with Teflon. The anodic CGDE process was stopped for 20 s every 30 min, and 0.5 mL samples of the reaction solution were taken each time from the sampling hole in the rubber plug. The products in the samples, as well as the unreacted starting material, were analysed using high-performance liquid chromatography (HPLC, Agilent 1100) using a Shodex RSpak KC-811 column and ultraviolet–visible (UV–VIS, 210 nm) spectroscopy (Agilent G1314A VWD). A Shodex RSpak KC-811 column was used to determine the concentration of formic acid (FA). In addition, a Shodex Ionpak ion chromatography (IC) I-524A column was used together with a conductivity detector (Shimadzu CDD-6A) for the analysis of chloride ions. The TOC in the solution was measured using a TOC analyser (Shimadzu TOC-VE). The products were identified by IC, HPLC and gas chromatography (GC)-mass spectrometry (MS).

To carry out the simultaneous degradation of TCA via combined anodic and cathodic degradation, the glass tube and the N117 membrane were not employed, as shown in Fig. 1ii. Instead, the cathode was directly immersed into the reaction solution containing TCA. Thus, TCA could also be transferred to the surface of cathode and reduced by the $\cdot H_{ads}$ adsorbed on the surface of the cathode, such as the Pd-loaded Ni-plate cathode. The anodic CGDE and the normal electroreduction process all took place in the glass cell. A voltage of 500 V from a direct current (DC) power supply (ELEPOS PS-1510) was also

applied between both electrodes to start the run of anodic CGDE in the cell. The depth of the discharge electrode (anode) dipped into solution was also adjusted so that the average current was 70 mA.

To investigate the cathodic degradation of TCA via the reductive action of the cathode, the apparatus shown in Fig. 1iii was employed. For cathodic degradation the cathode was placed in the cell and immersed in the reaction solution (70 mL) containing 5 mM TCA and 20 mM sodium sulfur, and the anode was introduced into the glass tube plugged with N117 and in contact with the electrolyte containing 20 mM sodium sulfur (5 mL) without TCA. Before each run, argon gas was passed through the solution to purge air from the cell. The anodic CGDE took place in the glass tube, while the normal electroreduction process took place in the glass cell. To start the run,a voltage of 500 V from a direct current (DC) power supply (ELEPOS PS-1510) was also applied between both electrodes and the current was also about 70 mA. Other factors, such as the cathode material, amount of Pd loaded onto the cathode, length of the anode dipped in the electrode, and catalyst Fe^{2+}, were also investigated.

Results and Discussion

The Effect of the Cathode Materials on the Simultaneous Degradation of TCA

To carry out the simultaneous degradation, the cathode should be directly introduced into the anodic CGDE as shown in Fig. 1ii. This allows the reductive ability of the cathode to be used for the reduction of TCA. Because the reduction of TCA by the action of the cathode is affected by the cathode material, three different cathode materials (Ni, stainless steel (St), and Cu) were employed to investigate the simultaneous degradation of TCA. In the case of anodic degradation, the cathode was separated from the anodic zone by N117 membrane, meaning that the cathode would not reduce the substrates in the anodic zone. For comparison, the results of the anodic degradation of TCA are shown in Fig. 2, and the test results using this setup are labelled N117.

For Cu, Ni, St, and N117 cathodes, the TCA removal rates for simultaneous degradation were 77.59%, 82.87%, 74.08%, and 65.32% respectively, the rates of the dechlorination TCA were 71.15%, 73.08%, 69.07%, and 62.03%, respectively, and the TOC reduction rates were 67.34%, 69.77%, 65.54%, and 64.6%, respectively, as shown in Fig. 2a. Of the tested cathodes, the N117 cathode showed the lowest performance, which could be because the cathode was separated from the anodic zone and no reduction of TCA occurred. These results indicate that the combination of anodic and cathodic degradations could enhance the degradation of TCA by anodic CGDE. Aside for the reduction in TOC, similar results were found for the cathodic degradation of TCA by the different cathode materials, as shown in Fig. 2b. In the case of the Ni cathode, the highest TCA removal and dechlorination rates were obtained. These results support the idea that, in simultaneous degradation, the reductive ability of the cathode strongly affects the TCA removal and dechlorination rates. Thus, the Ni cathode, which showed the highest reductive ability, was employed for the subsequent investigations.

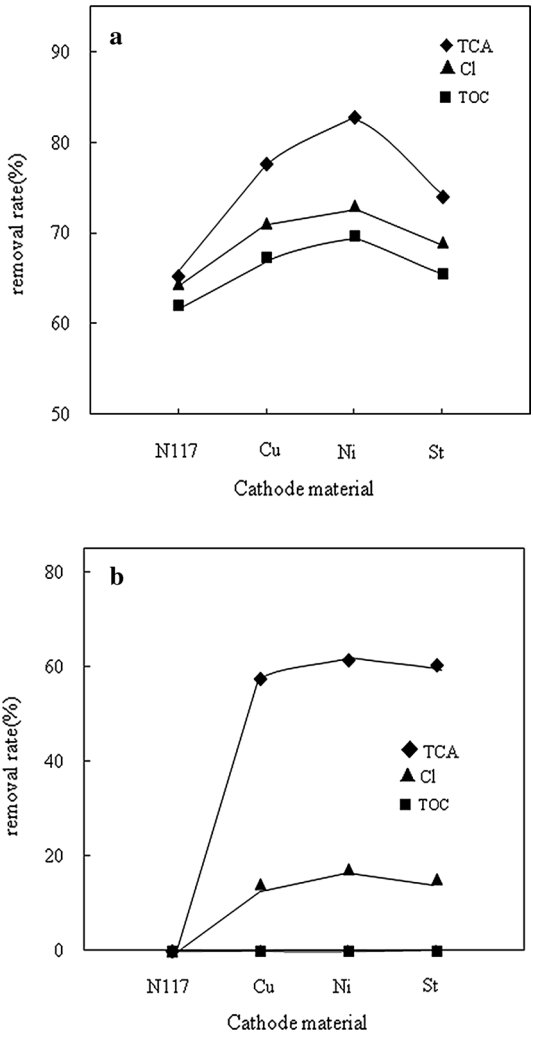

Fig. 2 **a** Effect of cathode materials on the simultaneous degradation of TCA ($C_0 = 5$ mM, $TOC_0 = 120.1$ ppm). **b** Effect of cathode materials on the reduction of TCA ($C_0 = 5$ mM, $TOC_0 = 120.1$ ppm)

The Effect of Length of the Anode Dipped in the Electrode

In simultaneous degradation, active species, such as ·OH and $\cdot H/e^-_{aq}$, are generated by the gas plasma and react with TCA. The gas plasma sustained by DC glow discharge was formed around the anode immersed well inside the liquid electrolyte. Thus, the effect of the length of the anode immersed in the electrode was investigated. For sustaining the anodic CGDE/gas plasma, the length of the anode dipped into the electrode should be in the range of 0.5 to 2.5 mm, corresponding to currents from about 40 to 80 mA. Furthermore, as the length of the anode immersed in the electrode increased, the current also increased, as shown in Fig. 3. Once the length of the anode dipped was greater than 2.5 mm, anodic CGDE ceased. This observation could be explained by the idea that, as the length of the anode immersed in the electrolyte increases, the Joule heating of the anode required to sustain the vapor layer around the anode, which

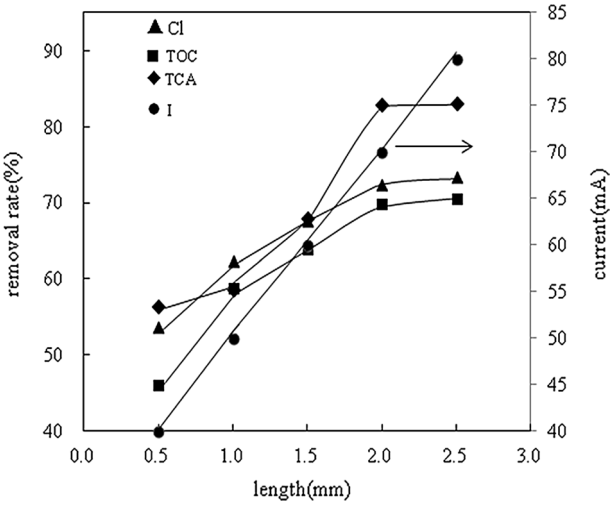

Fig. 3 The effect of the length of the anode dipped into the electrode on the simultaneous degradation of TCA (Ni cathode, $C_0 = 5$ mM, $TOC_0 = 120.1$ ppm)

is required for anodic CGDE, also increased [48]. The TCA and TOC reduction rates, as well as the dechlorination rate of TCA, also increased with increasing immersed length. In simultaneous degradation, a primary yield of 11 mol/(mol electron) each for ·H and ·OH in the liquid-phase reaction zone of anodic CGDE and a yield of 1 mol/(mol electron) for $\cdot H_{abs}$ on the cathode were obtained. Thus, as the length of the anode immersed in the electrolyte increased, greater concentrations of radicals including reductants ($\cdot H_{abs}$ and $\cdot H/e^-_{aq}$) and oxidants (·OH and H_2O_2) increased, resulting in higher removal and dechlorination rates [34].

Effect of Pd Loading

Pd and Ni are widely used as catalysts for the hydrogenation of chlorinated organic compounds [45, 46], and the activity for a given reaction can be improved significantly by using a mixed metal system [38]. Thus, Ni plates with different amounts of loaded Pd were employed as cathodes for the simultaneous degradation of TCA. The results are shown in Fig. 4. Once Pd had been loaded onto the Ni cathode, the removal rates and dechlorination rates of TCA increased markedly. This result can be rationalised by the idea that a mixed metal system can enhance the reductive ability of the cathodes [24]. In the mixed metal system, both the removal and dechlorination rates of TCA increased, reaching their highest values (91.82% and 80.12%, respectively) at a loading of approximately 0.4 mg/cm^2 Pd on Ni; subsequently, the removal rates decreased with further Pd loading. At lower Pd loadings, there was not enough highly reactive $\cdot H_{abs}$ bound to the Pd surface for dechlorination. At higher Pd loadings, the local current density for H^+ reduction was too high, resulting in excessive hydrogen gas evolution, thus disturbing the mass transfer of TCA to the surface of the Pd-loaded Ni cathode [38]. In the case of the TOC, a similar trend was obtained, but the variations were much smaller than those of TCA and dechlorination. This could be explained by the much longer mineralisation pathway for TCA than for the disappearance and dechlorination of TCA discussed in Sect. 3.6.

The simultaneous degradation of TCA with 0.4 mg/cm^2 Pd/Ni cathode was chosen as a standard, as shown in Fig. 5a–d. The two obvious gaps between the three degradation

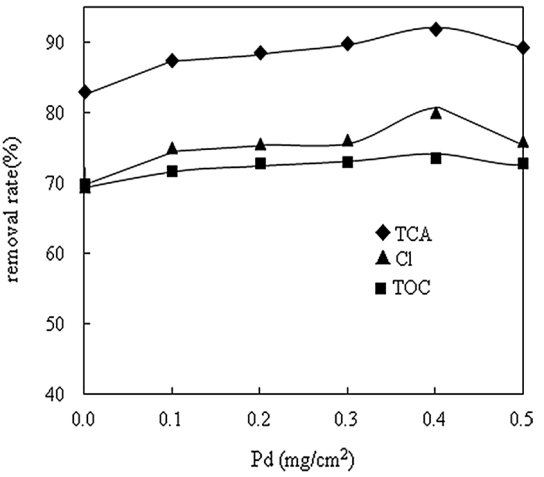

Fig. 4 Effect of Pd loading on the simultaneous degradation of TCA (C_0 = 5 mM, TOC_0 = 120.1 ppm)

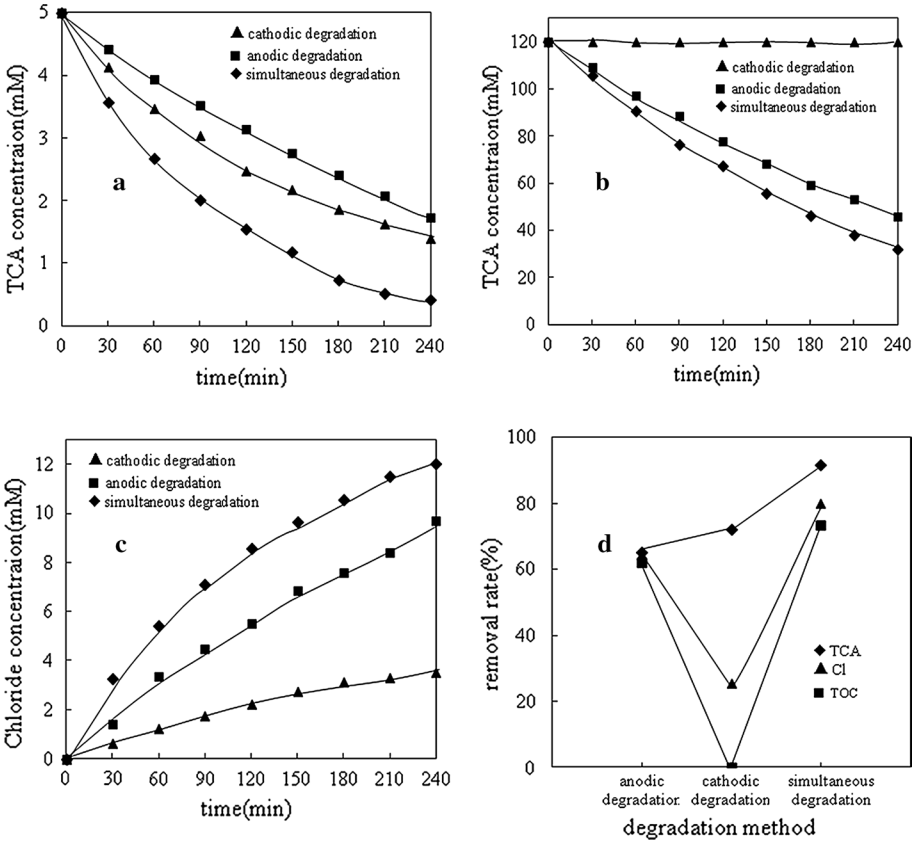

Fig. 5 **a** Degradation of TCA measured by three methods, **b** reduction in TOC by three methods, **c** dechlorination of TCA by three methods, and **d** removal rates for three methods at 240 min (0.4 mg/cm^2 Pd-loaded Ni cathode, distance between anode and cathode: 1.5 cm, pH_0 = 2.8, C_0 = 5 mM, TOC_0 = 120.1 ppm)

curves demonstrate the different TCA removal rates by the three methods. The simultaneous degradation of TCA was fastest: 91.82% and 73.03% reductions in TCA and TOC, respectively, and 80.12% of the chlorine atoms on TCA were released after 240 min with corresponding energy efficiencies of 9.11×10^{-6} M/kJ, 1.74×10^{-7} kg/kJ, and 2.38×10^{-5} M/kJ, respectively. For anodic degradation, 65.32% of the TCA and 62.03% of TOC were removed and 64.6% of the chlorine atoms on TCA were released after 240 min with corresponding energy efficiencies of 6.48×10^{-6} M/kJ, 1.48×10^{-7} kg/kJ, and 1.92×10^{-6} M/kJ, respectively. For cathodic degradation, 72.12% and 0% reductions in the TCA and TOC, respectively, were observed, and 25.6% of the chlorine atoms on TCA were released after 240 min with corresponding energy efficiencies of 7.16×10^{-6} M/kJ, 0 kg/kJ, and 0.76×10^{-5} M/kJ, respectively. Compared to anodic degradation, for the simultaneous degradation, the energy efficiencies of TCA and TOC reduction and the dechlorination of TCA increased by 40.5%, 17.8%, and 24.0%, respectively.

Characterisation of the Pd/Ni Electrode

$\cdot H_{abs}$ generated on the surface of the cathode is one of the reducing agents produced in simultaneous degradation. Because the generation of $\cdot H_{abs}$ is strongly affected by the surface of the cathode [36, 47], the surface structure of the Pd/Ni cathode was investigated. The surface morphology of the raw Ni plate was smooth, as shown in Fig. 6a. As shown in Fig. 6b, a film of clusters formed after electroless deposition of the Ni plate, indicating an increase in the surface area. Only diffraction peaks corresponding to Pd and Ni were found in the X-ray diffraction (XRD) patterns, as shown in Fig. 7. Thus, the Pd and Ni on the surface were present as a Pd/Ni bimetal and not a Pd/Ni alloy. Similar results have been reported by Yang and Ma separately [36, 47]. Based on these results, the main reaction site for the dechlorination of TCA is at the Pd surface or the interface of the Pd–Ni bimetallic phase. A mechanism of TCA dechlorination on the surface of Pd/Ni plate cathode is proposed in Sect. 3.6.

Effect of Fe^{2+} on the Simultaneous Degradation of TCA

The concentration of H_2O_2 generated in the anodic zone by anodic CGDE reached 33.4 mM without organic substrates. TCA could not be directly degraded by H_2O_2 in this work. Because H_2O_2 could be converted to ·OH by Fe^{2+} as a catalyst [as shown in reaction

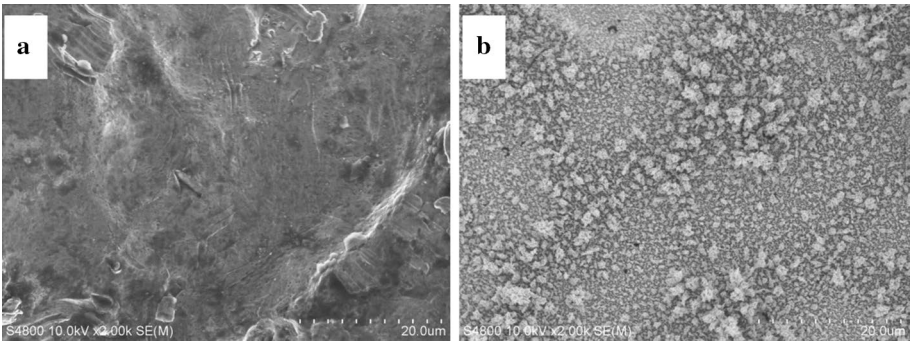

Fig. 6 **a** SEM images of a Ni plate cathode and **b** Pd/Ni plate cathode (0.4 mg/cm^2 Pd-loaded Ni cathode)

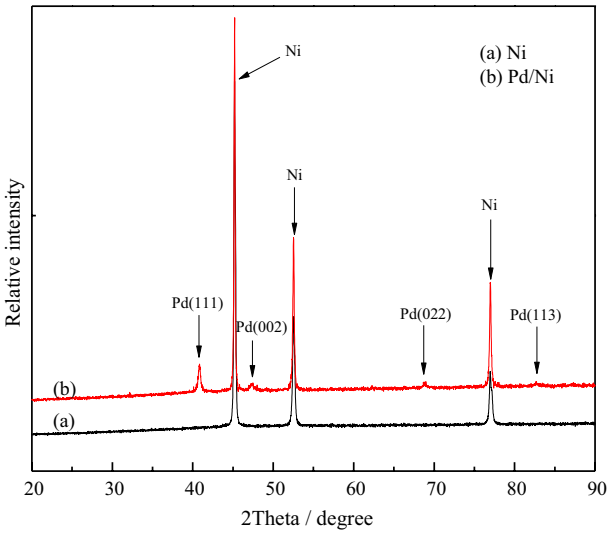

Fig. 7 XRD patterns of the Pd/Ni plate cathode (0.4 mg/cm^2 Pd-loaded Ni cathode)

(5)] [36], to enhance the efficiency of TCA removal, Fe^{2+} was added to investigate its effect on the anodic degradation of TCA. Once Fe^{2+} had been added, the removal rates increased, as shown in Fig. 8. When the concentration of Fe^{2+} was 3.75 mM, the TCA and TOC reduction rates and the dechlorination rates of TCA were 93.99%, 73.45%, and 82.46%, respectively, with corresponding energy efficiencies of 9.34×10^{-6} M/kJ, 1.75×10^{-7} kg/kJ, and 2.45×10^{-5} M/kJ. These results might be rationalised by the idea that Fe^{2+} could convert H_2O_2 to ·OH, thus enhancing the concentration of ·OH and allowing ·OH attack and the direct decomposition of TCA.

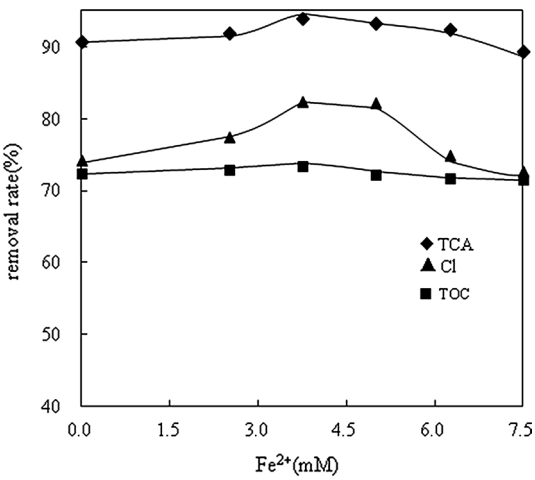

Fig. 8 Effect of Fe^{2+} on the simultaneous degradation of TCA (0.4 mg/cm^2 Pd-loaded Ni cathode, $C_0=5$ mM, $TOC_0=120.1$ ppm)

Table 1 Intermediate products in the degradation of TCA using the three degradation methods

Methods	Intermediate products			
Anodic degradation	$Cl_2CHCOOH$ (DCA)	$ClCH_2COOH$ (MCA)	CH_3COOH (AA)	HCOOH (FA)
Cathodic degradation	$Cl_2CHCOOH$ (DCA)	$ClCH_2COOH$ (MCA)	CH_3COOH (AA)	
Synergistic degradation	$Cl_2CHCOOH$ (DCA)	$ClCH_2COOH$ (MCA)	CH_3COOH (AA)	HCOOH (FA)

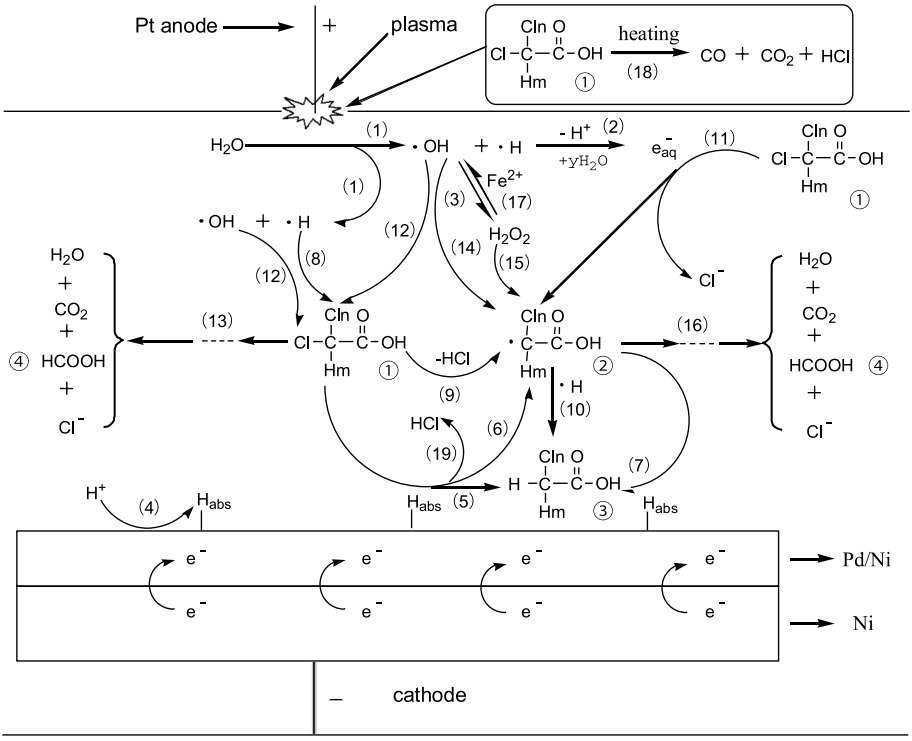

Fig. 9 Possible simultaneous degradation pathways (m, $n \in (0, 1, 2)$, $m+n=2$)

Intermediate Products and Possible Degradation Pathways

To obtain further information about the degradation process, the intermediates formed in the degradation of TCA by the three methods were investigated. The results are tabulated in Table 1. The variation in the concentrations of the intermediates is shown in Fig. 10a–c. In all three methods, Cl^- was detected as a product, and CO_2 was found as a product of both anodic degradation and simultaneous degradation. Though the products labelled ② (DCA·, MCA·, and AA·) were not detected, products ② should be intermediate products [34, 38]. Based on the results, possible anodic, cathodic, and simultaneous degradation pathways for simultaneous degradation are proposed (see Fig. 9). There are total eighteen possible reactions.

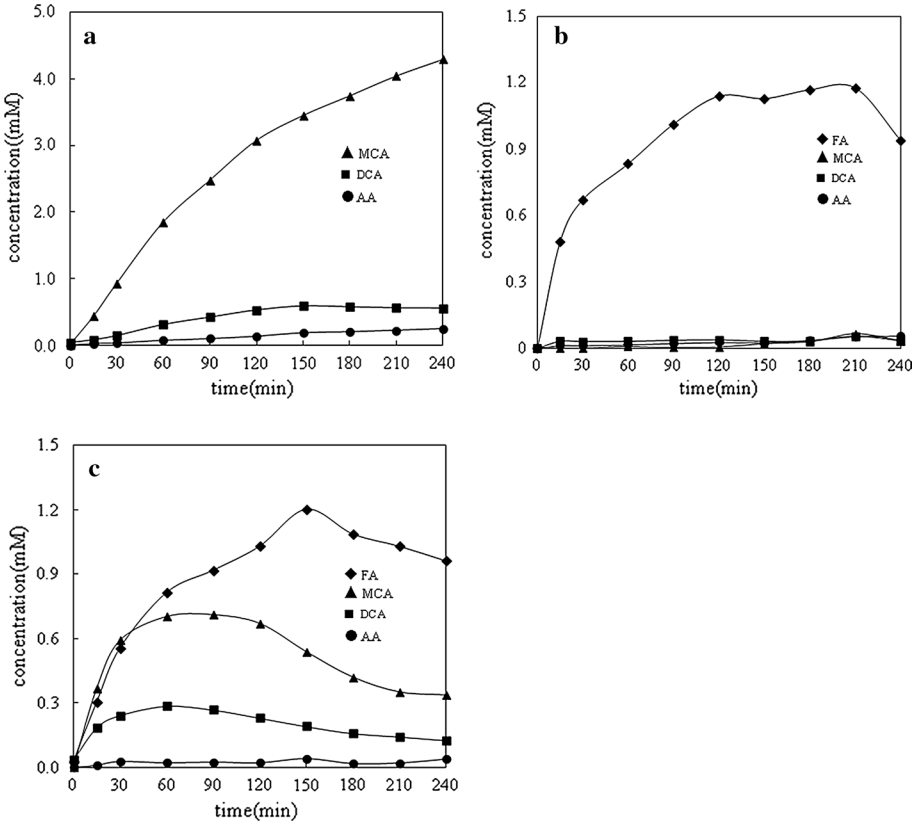

Fig. 10 **a** The variation in the concentrations of the intermediates in cathodic degradation. **b** The variation in the concentrations of the intermediates in anodic degradation. **c** The variation in the concentrations of the intermediates in simultaneous degradation (TCA, $C_0 = 5$ mM, $TOC_0 = 120.1$ ppm)

In cathodic degradation, significant quantities of DCA, MCA, and AA were found as intermediates (see Fig. 10a). The generation of these species is a result of the reduction of the corresponding substrates ① (TCA, DCA, and MCA) by $\cdot H_{ads}$ on the surface of the Pd-loaded Ni cathode via pathway I containing reaction (5), and pathway II containing reactions (6) and (7), as shown in Fig. 9. Substrates ② should be formed in reaction (6). In addition, $\cdot H_{ads}$ should be generated by the reduction of H^+ on the surface of Pd/Ni cathode through pathway III containing reaction (4). As shown in Fig. 10a, the concentration of MCA was much higher than that of DCA, indicating that MCA was much less susceptible to reduction than DCA.

For anodic degradation, DCA, MCA, AA, and FA were detected as intermediate products (see Table 1 and Fig. 10b). The concentrations of DCA, MCA, and AA were significantly lower than those in cathodic degradation, as shown in Fig. 10a, b. This indicates that there were also reduction reactions of the substrates in the anodic degradation of TCA [34]. The generation of DCA, MCA, and AA might result from the reduction of substrates ① and ② by ·H and/or e_{aq}^- through two different reaction pathways: pathway IV containing reactions (8), (9), and (10), and pathway V containing reactions (11) and (10), respectively. The concentration of FA was an order of magnitude larger than those of DCA, MCA, and

AA. The formation of FA might be explained by the oxidative degradation of substrates ① and ② by ·OH and/or H_2O_2 through two different reaction pathways: pathway VI containing reactions (12) and (13) and pathway VII containing reactions (14) and/or (15) and (16). Although the formation of FA might be mainly from the oxidation of TCA based on the low concentration of DCA, MCA, and AA. The direct oxidative degradation of TCA by H_2O_2 was not observed in our experiments. Although H_2O_2 could be converted to ·OH by the Fenton reaction and TCA oxidised by ·OH via pathway VIII containing reactions (17) and (12) [39], considering the concentrations of DCA, MCA, and AA were significantly lower than that of FA, reduction reaction pathways IV and V are less important than oxidation reaction pathways VI and VII for the anodic degradation of TCA. Though the concentration of CO was too low to be quantified, it was detected by GC–MS, indicating the existence of reaction pathway IX containing reaction (18) in the thermal decomposition of TCA. However, pathway IX is not very important for the anodic degradation of TCA [34].

In simultaneous degradation, DCA, MCA, AA and FA were also found to be the primary intermediates. The concentrations of DCA, MCA, and AA were higher than those in anodic degradation (see Fig. 10b, c). This can be explained by the idea that the formation of DCA, MCA, and AA might not only occur through pathways IV and V in anodic degradation but also through pathways I and II in cathodic degradation. Furthermore, as shown in Fig. 10c, the formation of DCA, MCA, and AA in simultaneous degradation should be due to the cathodic reduction of TCA, DCA, and MCA (via pathway I). The highest concentration of FA was formed via simultaneous degradation, and the concentrations were almost the same in anodic degradation.

The simultaneous degradation of TCA might be triggered in three ways: (1) the abstraction of chlorine from TCA by ·OH [see reaction (12)]; (2) the reduction of TCA by $\cdot H/e^-_{aq}$ [see reactions (8) and (11)]; and (3) the reduction of TCA by $\cdot H_{ads}$ [see reactions (5) and (6)], resulting in the formation of corresponding intermediates [(1) and (2)] and the release of Cl^-. Based on the discussion above, it seem that routes (1) and (3) might be more important than (2). Because (1) and (2) occur in anodic degradation and (3) occurs in cathodic degradation, the existence of an additive effect of cathodic and anodic degradations on TCA removal could occur in simultaneous degradation. Further oxidative degradation and mineralisation of the intermediate products (such as substrates ②) by the attack of ·OH or H_2O_2 would result in a reduction in TOC. Both further reductive and oxidative degradation of the chlorinated intermediates products would lead to their dechlorination. Because chlorinated intermediates could be generated through all three routes mentioned above in simultaneous degradation, synergistic cathodic and anodic degradations for both the reduction in TOC and dechlorination could occur in the simultaneous degradation process.

Kinetics of TCA Degradation

The TCA decay curves in the three degradation methods are shown in Fig. 5a, and these plots show exponential degradation. Consequently, we fitted the data to the integral rate equation for the first-order reaction, as Eq. (5):

$$\ln\left(C_0/C\right) = kt, \tag{5}$$

where C, C_0, k, and t denote the concentration of TCA at the given reaction time, that at $t=0$, the rate constant, and the reaction time, respectively.

In consequence, for each set of data concerning decay, a straight line with good correlation was obtained, as shown in Fig. 11a. This result indicates that TCA reacted per the

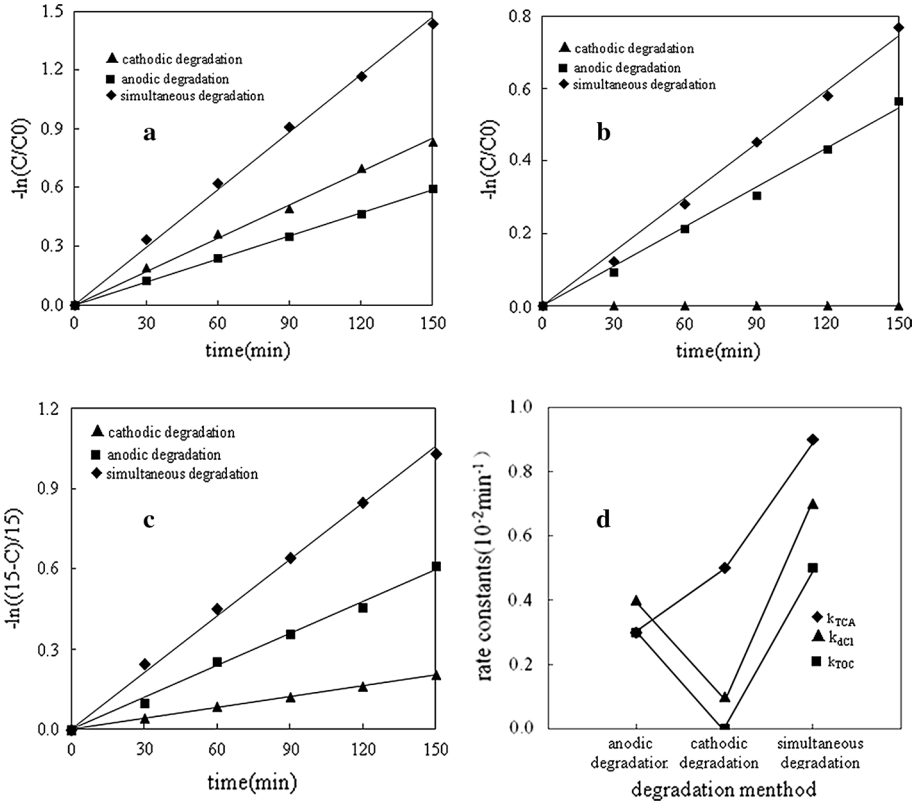

Fig. 11 **a** First-order plots for the degradation of TCA (C_0: 5.0 mmol/L), **b** first-order plots for the decay of TOC (120.1 ppm), **c** first-order plots of the dechlorination of TCA (C_0: 5.0 mmol/L), and **d** the apparent rate constants

first-order rate law in the three different methods. The apparent rate constants, k_{TCA}, for the decay of TCA were calculated from the slopes of each line to be $k_{SD\ (TCA)} = 8.7 \times 10^{-3}$ min^{-1} for simultaneous degradation, $k_{AD\ (TCA)} = 3.4 \times 10^{-3}$ min^{-1} for anodic degradation, and $k_{CD\ (TCA)} = 5.4 \times 10^{-3}$ min^{-1} for cathodic degradation. The value of $k_{SD\ (TCA)}$ is obviously larger than either $k_{AD\ (TCA)}$ or $k_{CD\ (TCA)}$, meaning that a combination of the action of anodic CGDE and normal electrolytic processes at the cathode could efficiently enhance the TOC reduction rate. The value of $k_{SD\ (TCA)}$ (0.87×10^{-3} min^{-1}) is almost equal to the sum of $k_{AD\ (TCA)}$ and $k_{CD\ (TCA)}$ (0.88×10^{-3} min^{-1}). This means that the simultaneous degradation of TCA might be an additive effect of the cathodic and anodic degradation processes.

As shown in Fig. 5b, except for cathodic degradation, the TOC disappearance curves for the other two methods are exponential over the course of the reaction, and these data were also fitted to Eq. (5). As expected, for each set of data concerning the decay, a straight line with good correlation was obtained, as shown in Fig. 11b. This result indicates that the TOC also decayed in accordance with the first-order rate law. The apparent rate constants, k_{TOC}, for the decay of TOC were calculated from the slope of each line to be $k_{SD\ (TOC)} = 5.2 \times 10^{-3}$ min^{-1} for simultaneous degradation, $k_{AD\ (TOC)} = 3.1 \times 10^{-3}$ min^{-1} for

anodic degradation, and $k_{CD\ (TOC)} = 0 \times 10^{-3}$ min^{-1} for cathodic degradation. $k_{SD\ (TOC)}$ was much larger than the sum of $k_{AD\ (TOC)}$ and $k_{CD\ (TOC)}$, indicating that the reduction in TOC is an effect of the synergistic cathodic and anodic degradation processes. The reduction in TOC could be due to the oxidative reaction of substrates such as MCA and DCA in anodic degradation. For MCA, DCA, and TCA, the TOC reduction rates decreased in the following order: $k_{AD\ (TOC\ of\ MCA)}$ $(10.4 \times 10^{-3}) > k_{AD\ (TOC\ of\ DCA)}$ $(10.1 \times 10^{-3}) > k_{AD\ (TOC\ of\ TCA)}$ (3.1×10^{-3}) in anodic degradation. For simultaneous degradation, a significant amount of MCA and DCA were generated from TCA by cathodic degradation, and MCA and DCA were oxidised and mineralised to CO_2 by anodic degradation, resulting in a higher TOC reduction rate than that in anodic degradation.

Because the formation of Cl^- on the oxidation of TCA should follow simple exponential growth kinetics, as Eq. (6) [49],

$$C = C_T[1 - \exp(-k_{Cl}t)], \tag{6}$$

and the dechlorination of TCA should follow Eq. (7).

$$\ln[(C_T - C)/C_T] = -tk_{dCl} \tag{7}$$

Here C_T is the starting concentration of chlorine atoms in TCA, and the final concentration of chloride (i.e., 15 mM), C is the chloride concentration at time t, k_{dCl} is the dechlorination rate, and k_{Cl} is the rate of chloride formation ($k_{dCl} = -k_{Cl}$).

When the kinetic data were plotted according to Eq. (7), a straight line with a satisfactory correlation coefficient was obtained, as shown in Fig. 11c. This suggests that the dechlorination of TCA followed the first-order rate law. The apparent rate constant, k_{dCl}, for the dechlorination of TCA was calculated from the slope of the corresponding line to be $k_{SD\ (dCl)} = 7.1 \times 10^{-3}$ min^{-1} for simultaneous degradation, $k_{AD\ (dCl)} = 4.3 \times 10^{-3}$ min^{-1} for anodic degradation, and $k_{CD\ (dCl)} = 0.9 \times 10^{-3}$ min^{-1} for cathodic degradation. The value of $k_{SD\ (dCl)}$ was obviously larger than the sum of $k_{AD\ (dCl)}$ and $k_{CD\ (dCl)}$. Thus, for the simultaneous dechlorination of TCA, the cathodic and anodic degradation processes were synergistic. In addition to the dechlorination of TCA caused by the anodic and cathodic degradation of TCA, the synergistic effect on dechlorination might also be due to the mineralisation of the chlorinated intermediates, such as MCA and DCA, resulting in a higher dechlorination rates than those in single anodic degradation and single cathodic degradation.

Conclusions

TCA could be successfully decomposed and converted to inorganic products by the combination of the action of anodic CGDE and the normal electrolytic processes at the cathode. The chlorine atoms in the TCA were liberated as chloride ions. The disappearance of TCA and TOC, as well as the dechlorination of TCA, followed first-order kinetics. Compared with anodic degradation and cathodic degradation processes, simultaneous degradation resulted in an increase in the dechlorination rate of TCA, as well as increases in the TCA and TOC reduction rates. The simultaneous degradation of TCA might occur in the following manner: first, the degradation of TCA is triggered by the electrophilic attack of ·OH and reduction by $\cdot H_{ads}$ and $\cdot H/e^-_{aq}$, resulting in the corresponding intermediates and the release of Cl^-. Subsequently, further oxidative degradation via the attack of ·OH and H_2O_2 results in the formation of carboxylates and, finally, mineralisation to inorganic carbon. In the simultaneous degradation of TCA, there may be an additive effect of the anodic and cathodic degradation processes, whereas, in the simultaneous reduction in TOC and dechlorination of TCA, the anodic and cathodic degradation processes might be

synergistic. The efficient removal of TCA by our method demonstrates it potential for use in the treatment of other chlorinated organic compounds.

Acknowledgements This work was supported by the National Natural Science Foundation of China (Grant No. 51308276); Scientific Research Foundation for Doctors of Liaoning Province (Grant No. 20141123); Growth Plan for Distinguished Young Scholars in Colleges and Universities of Liaoning Province China (LJQ2015055); Anshan Science and Technology Program Project (Grant No. 2961); the National Natural Science Foundation of China (51102126); Innovative Research Team in Colleges and Universities of Liaoning Province China (LT2014007); and Natural Science Foundation of Liaoning Province, China (2015020634). Special thanks go to Professor Meguru Tezuka (Saitama Institute of Technology) and Professor Lifen Liu (Dalian University of Technology) for their comments and support.

References

1. Bruggeman PJ (2016) Plasma Sources Sci Technol 25:053002
2. Wang BJ, Wu YF, Jiang BC, Song HO, Li WT, Jiang YL, Wang CM, Sun L, Li Q, Li AM (2016) Electrochim Acta 219:509
3. Dabo P, Cyr A, Laplante F, Jean F, Menard H, Lessard J (2000) Environ Sci Technol 34:1265
4. Wang XY, Zhou MH, Jin XL (2012) Electrochim Acta 83:501
5. Miyoshi K, Kamegaya Y, Matsumura M (2004) Chemosphere 56:187
6. Hickling A, Ingram MD (1964) Trans Faraday Soc 60:783
7. Sengupta SK, Singh OP (1991) J Electroanal Chem 301:189
8. Sengupta SK, Singh OP (1994) J Electroanal Chem 369:113
9. Sengupta SK, Singh R, Srivastava AK (1998) Indian J Chem 37A:558
10. Singh R, Gangal U, Sen Gupta SK (2012) Plasma Chem Plasma Process 32:609
11. Srivastava Y, Jaiswal S, Singh OP, Sen Gupta SK (2014) Indian J Chem 53A:62
12. Buxton GV, Greenstock CL, Helman WP, Ross AB (1998) Phys Chem Ref Data 17:513
13. Gangal U, Srivastava M, Sen Gupta SK (2010) Plasma Chem Plasma Process 30:299
14. Tomizawa S, Tezuka M (2007) Plasma Chem Plasma Process 27:486
15. Lu QF, Yu J, Gao JZ (2006) J Hazard Mater B136:526
16. Liu YJ (2009) J Hazard Mater 166:1495
17. Wen YZ, Jiang XZ, Liu WP (2002) Plasma Chem Plasma Process 22:175
18. Amano R, Tezuka M (2006) Water Res 40:1857
19. Jin XL, Zhang HM, Wang XY, Zhou MH (2012) Electrochim Acta 59:474
20. Wang L, Liu P, Zhang S (2015) Electrochim Acta 165:390
21. Wang L, Liu P, Chen T (2016) Plasma Chem Plasma Process 36:615
22. Gao J, Chen L, He YY, Yan ZC, Zheng XJ (2014) J Hazard Mater 265:261
23. Jin X, Wang X, Wang Yu, Ren H (2013) Ind Eng Chem Res 52:9726
24. Hong S, Min ZW, Mok C, Kwon H, Kim T, Kim D (2013) Food Sci Biotechnol 22:1773
25. Tong S, Ni Y, Shen C, Wen Y, Jiang X (2011) Water Sci Technol 63:2814
26. Bae JS, Lee JS, Kim YS, Sim WJ, Lee H, Chun JY, Park K (2008) Korean Chem Eng Res 46:886
27. Munegami T, Shimoyama A (1998) Viva Origino 26:103
28. Sen Gupta SK (2017) Plasma Chem Plasma Process 37:897
29. Yang HM, Matsumoto Y, Tezuka M (2009) J Environ Sci 21:142
30. Yang HM, Tezuka M (2011) J Phys D Appl Phys 44:155203
31. Yang HM, Tezuka M (2011) J Environ Sci 44:231044
32. Yang HM, Cai X, Tezuka M (2013) Plasma Chem Plasma Process 33:1043
33. Wang L, Jiang XZ (2008) Environ Sci Technol 42:8492
34. Wang L, Zeng H, Yu X (2014) Electrochim Acta 115:332
35. Rumbach P, Go DB (2017) Synth Top Catal 60:799
36. Gong JY, Wang J, Xie WJ, Cai WM (2008) J Appl Electrochem 38:1749
37. Zhao YL, Li XF (2011) Environ Chem 1:20
38. Melnick RL, Nyska A, Foster PM, Roycroft JH, Kissling GE (2007) Toxicology 230:126
39. McRae BM, LaPara TM, Hozalski RM (2004) Chemosphere 55:915
40. Lifongo LL, Bowden DJ, Brimblecombe P (2004) Chemosphere 55:467
41. Yang HM, Zhao XT, An BA, Li LX, Wang SY, Ju MW (2017) Environ Protect Chem Ind 4:404
42. Wu C, Wei D, Fan J, Wang L (2001) Chemosphere 44(5):1293
43. Kosobutskii VS (2001) High Energy Chem 35(3):202
44. Thagard SM, Stratton GR, Dai F, Bellona CL, Holsen TM, Bohl DG, Paek E, Dickenson ER (2017) J Phys D Appl Phys 50:014003

45. Scialdone O, Corrado E, Galia A, Sirés I (2014) Electrochim Acta 132:15
46. Hu B, Wu C, Zhang Z, Wang L (2014) Ceram Int 40(5):7015
47. Tsyganok AI, Otsuka K (1998) Electrochim Acta 43:2589
48. Sen Gupta SK (2015) Plasma Sources Sci Technol 24:063001
49. Minero C, Aliberti C (1991) Langmuir 7:928